Chemical Science

RSC Publishing

EDGE ARTICLE

View Article Online
View Journal | View Issue

# Metal ions triggered ligase activity for rolling circle amplification and its application in molecular logic gate operations†

Cite this: *Chem. Sci.*, 2013, **4**, 1858

Sai Bi,[ab] Bin Ji,[b] Zhipeng Zhang[b] and Jun-Jie Zhu*[a]

Received 6th January 2013
Accepted 4th February 2013

DOI: 10.1039/c3sc00043e

www.rsc.org/chemicalscience

Supramolecular structures composed of padlock probes and primers were used to perform rolling circle amplification (RCA) which was achieved by metal ion ($Hg^{2+}$ or $Ag^{+}$) induced DNA ligase activity. In the presence of $Hg^{2+}$ (or $Ag^{+}$), the specific and strong interaction between thymidine–thymidine and $Hg^{2+}$ (or cytosine–cytosine and $Ag^{+}$) at the terminal of the padlock probe enabled the circularization of the padlock probe with primer in the aid of DNA ligase. An RCA process was then accomplished by DNA polymerase/dNTPs. The RCA product containing multiple tandem repeats could hybridize with a large number of molecular beacons (reporter), resulting in an enhanced fluorescence signal. This proposed single-input YES gate enabled the sensitive and selective detection of $Hg^{2+}$ (or $Ag^{+}$). Additionally, based on the principle of DNA hybridization and displacement, a NOT logic gate was constructed by designing a double-stranded fluorescence probe as reporter. Significantly, this assay was further applied to the construction of a complete set of two-input molecular-scale logic gates and three advanced logic devices.



## Introduction

So far, particular attention has been paid for the monitoring of metal ions owing to their severe effects on human health and environment.[1] Therefore, highly sensitive and selective detection of different ions in water and food resources is of great significance for the management and prevention of ion pollution.[2]

Recently, the interaction between metal ions and DNA base pairs has attracted growing interest due to its great potential in sensing applications. For example, a class of nucleic acids possessing specific binding properties towards certain metal ions (aptamers) or the catalytic nucleic acids selectively incorporating with metal ions as cofactors (DNAzymes or ribozymes) were selected by the SELEX (systematic evolution of ligands by exponential enrichment) process or *in vitro* selection.[3] Moreover, it has been well demonstrated that various metal ions can specially bridge nucleosides or ligandosides to form stable metal-ion-coordinated base pairs. Prominent examples include $Hg^{2+}$ specifically and strongly binding to a thymine–thymine (T–T) mismatch in DNA duplexes to form stable T–$Hg^{2+}$–T base pairs,[4] while $Ag^{+}$ binds to two cytosine (C) bases to form C–$Ag^{+}$–C complexes.[5] These features provide a new and versatile platform for the construction of molecular machines for metal ions detection,[6] and even the performance of logic gates.[7] Most representatively, Willner *et al.* developed T-rich or C-rich functionalized CdSe/ZnS quantum dots (QDs) for the multiplexed optical analysis of $Hg^{2+}$ or $Ag^{+}$, which were further used for logic gate operations (YES, AND and OR).[8] Additionally, Park's group constructed a molecular-scale logic gate system that used $Hg^{2+}$ or $Ag^{+}$ ions as inputs to form T–$Hg^{2+}$–T or C–$Ag^{+}$–C base pairs with a template to perform the PCR amplification as an output (YES, PASS1, AND and OR).[9] Undoubtedly, these logic gates were cost-effective and had easy operation. However, they were still limited with respect to the sensitivity and integrity of a logic gate system. Therefore, it is highly desirable to develop a complete set of logic gates that can operate in a more sensitive and selective manner.

Rolling circle amplification (RCA) is a popular isothermal amplification method allowing the polymerase-mediated replication of a circular template primed by a single-stranded nucleic acid to create long DNA concatemers.[10] The RCA products with repetitive sequence units can be labeled with multiple fluorophores,[11] enzymes,[12] and nanoparticles,[13] thereby amplifying the signal generated from a single target molecule to a level that can be detected. Due to the simplicity, robustness and high signal amplification, RCA has been widely employed in quantification of various targets, such as RNA,[14] DNA,[15] protein[16] and so on.[17] However, few studies have been reported, so far, on employing RCA for metal ions detection.

[a]*State Key Laboratory of Analytical Chemistry for Life Science, School of Chemistry and Chemical Engineering, Nanjing University, Nanjing 210093, P. R. China. E-mail: jjzhu@nju.edu.cn; Fax: +86-25-83597204; Tel: +86-25-83597204*

[b]*Key Laboratory of Biochemical Analysis, Ministry of Education, College of Chemistry and Molecular Engineering, Qingdao University of Science and Technology, Qingdao 266042, P. R. China*

† Electronic supplementary information (ESI) available: Detection of $Ag^{+}$ and detailed diagrammatic representation, fluorescence results and truth table of OR, INHIBIT, XOR, NAND, NOR, and XNOR logic operations. See DOI: 10.1039/c3sc00043e

Herein, a T–$Hg^{2+}$–T or C–$Ag^{+}$–C mediated RCA strategy was proposed for highly sensitive and selective detection of $Hg^{2+}$ or $Ag^{+}$, which was further developed for the construction of a complete set of two-input molecular-scale logic gates and advanced logic devices. It should be noted that two kinds of signalling probes were employed to transduce the logic operations. One was the stem-loop-structured fluorescent molecular beacon (MB) used to execute the YES, AND, OR, XOR, and INHIBIT operations, while the other was a double-stranded fluorescent probe to construct the NOT, NAND, NOR, and XNOR gates based on the principles of DNA hybridization and displacement reaction. To the best of our knowledge, this is the first report by using RCA for sensitive and selective detection of metal ions based on the specific interactions of ions with nucleic acids, let alone by using metal ions as inputs and RCA products as outputs to construct logic gates.

## Results and discussion

### YES and NOT gates for $Hg^{2+}$ (or $Ag^{+}$) detection

Firstly, take the detection of $Hg^{2+}$ for example (Fig. 1A). Padlock probe (1) is designed to form T–T mismatch with primer (2) at its 5′ end. In this case, the terminal mismatching blocks the activity of T4 DNA ligase at the 5′ end, which prevents the ligation and circularization of padlock probe (1) with the primer (2) as the template even in the presence of DNA ligase. Upon the addition of $Hg^{2+}$, the terminal T–T mismatched oligonucleotides can cooperatively coordinate with $Hg^{2+}$ to form a non-natural but stable T–$Hg^{2+}$–T complex. This precise hybridization of padlock to the primer makes the 3′ and 5′ ends of padlock adjacent, which induces the activity of the DNA ligase. As a consequence, the padlock probe (1) is specifically ligated and circularized with the primer (2) by DNA ligase. Subsequently, an RCA reaction is conducted in the presence of DNA polymerase/dNTPs. It should be noted that to avoid the influence of $Hg^{2+}$ (or $Ag^{+}$) that is released during the RCA process, cysteine (Cys) is introduced to selectively coordinate with $Hg^{2+}$ (or $Ag^{+}$).[5a,18] The resulting RCA products with thousands of repetitive DNA domains make the molecular beacons (MBs) (3) open and restore their fluorescence due to the hybridization between the RCA product and MBs, achieving the utilization of RCA for the signal-on fluorescence detection of aqueous $Hg^{2+}$ (pathway a, Fig. 1A). This observation is consistent with the proper execution of a single-input YES gate that produces a fluorescent signal in response to an input ion (an output 0 from an input 0 and an output 1 from an input 1). Utilizing the present homogeneous assay, the target $Hg^{2+}$ can be sensitively detected in the range from 0.1 nM to 1.0 μM with a detection limit as low as 0.1 nM (Fig. 1B).

Moreover, based on the principle of DNA hybridization and displacement, a NOT logic gate is constructed by the same components as the YES gate but using a double-stranded fluorescence probe. As depicted in Fig. 1A pathway b, in the absence of $Hg^{2+}$, DNA (5) is perfectly complementary to the central bases of MB (4) with 17-mer to form the double-stranded probe with a fluorescence emission (output 1). There is still 11-mer overhang segment at 3′ end of DNA (5) for subsequent DNA displacement reaction through hybridization with the more complementary RCA products. Thus, when the gate is triggered by an $Hg^{2+}$ input, MB (4) is displaced and released by the resultant concatemeric RCA product, freeing it to a stable hairpin structure with a quenched fluorescence (output 0). In contrast to the YES logic gate, a fluorescent signal is observed in the absence of $Hg^{2+}$, while a decreased fluorescence emission is generated with the increase of $Hg^{2+}$ concentration (Fig. 1C), which performs the NOT logic operation.

To evaluate the selectivity of this assay for $Hg^{2+}$, a series of metal ions including $Ca^{2+}$, $Cd^{2+}$, $Fe^{3+}$, $K^{+}$, $Mg^{2+}$, $Mn^{2+}$, $Na^{+}$, $Ni^{2+}$, $Pb^{2+}$, $Zn^{2+}$, $Hg^{2+}$ and $Ag^{+}$ (each with a concentration of 1.0 μM) are tested for YES gate operation. As shown in Fig. 2, the appreciable fluorescence signal is only observed in response to $Hg^{2+}$ from the T–T mismatch, but hardly detects substantial signals to other metal ions. These results demonstrate an excellent selectivity of the proposed assay for $Hg^{2+}$ analysis against other environmentally relevant metal ions, attributed to the highly specific coordination of $Hg^{2+}$ ions to the corresponding mismatched base pair to form stable T–Hg–T bonding.

Similarly, the proposed strategy could also be used to sensitively and selectively detect $Ag^{+}$ on the basis of the specific interaction between $Ag^{+}$ and C–C mismatched to form a C–$Ag^{+}$–C complex. The results indicate that $Ag^{+}$ can be analyzed to a detection limit of 0.1 nM with an excellent selectivity for $Ag^{+}$ ions (see ESI†).

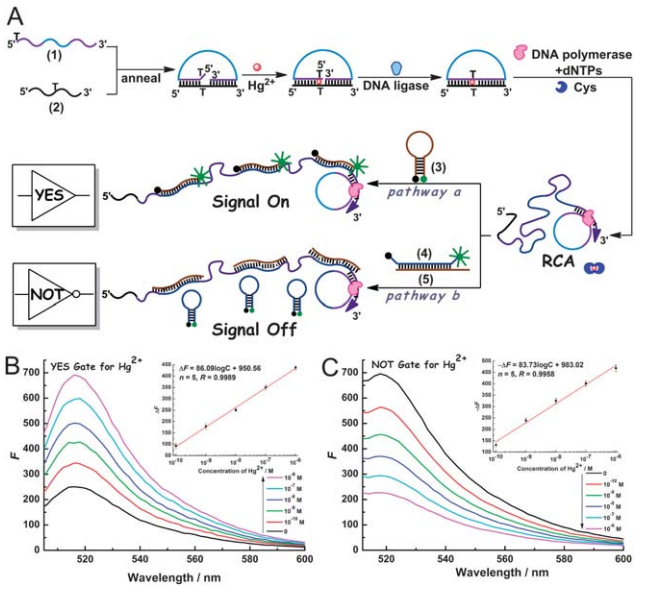


**Fig. 1** (A) Diagrammatic representation of DNA ligase activity triggered by $Hg^{2+}$, which further initiates RCA reaction in the presence of DNA polymerase/dNTPs. Molecular beacon (MB) probe (3) and double-stranded fluorescence probe (4 and 5) are employed as fluorescence reporters to perform "YES" gate (pathway a) and "NOT" gate (pathway b), respectively. MBs (3) and (4) are modified with fluorescein (FAM) and Dabcyl as a fluorophore/quencher coupled to the 5′- and 3′-end, respectively. Fluorescence quenching or emission of the system at $\lambda = 518$ nm is defined as a "false" output (0) or "true" output (1), respectively. (B and C) Fluorescence spectra of FAM corresponding to difference concentrations of $Hg^{2+}$ in "YES" gate and "NOT" gate, respectively. The arrows indicate the signal changes with increases in the $Hg^{2+}$ concentration (0, $10^{-10}$, $10^{-9}$, $10^{-8}$, $10^{-7}$, and $10^{-6}$ M). Insets: corresponding calibration curves for various concentrations of $Hg^{2+}$.

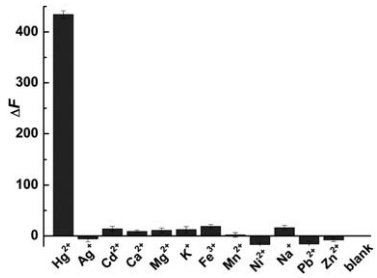


**Fig. 2** Selectivity of specific metal ions to trigger the DNA ligase activity. The sequences of padlock probe and primer are the same as those in Fig. 1A which contain a T–T mismatch. The concentration of each metal ion is 1.0 μM.



### AND logic gate

Accordingly, a complete set of two-input logic gates (AND, OR, INHIBIT, XOR, NAND, NOR, and XNOR) is constructed based on the above described methods by using $Hg^{2+}$ and $Ag^{+}$ ions as inputs. As shown in Fig. 3A, an AND gate is consisted of a padlock (1) and a primer (7), which obtains an output of 1 only when both inputs are held at 1. In this system, $Hg^{2+}$ and $Ag^{+}$ specifically interact with the mismatched T base pair and C base pair at the 5′ and 3′ ends of the padlock, respectively. Thus, when either of the two metal ions is present alone, only one end of padlock can be hybridized with the template, which still has a gap and cannot be sealed by DNA ligase. Only in the presence of the two inputs, can the DNA ligase be activated to make the padlock circular to facilitate the following RCA reaction that results in a fluorescent signal. The output fluorescence signals of the AND gate in the form of bars presentation and the corresponding truth table are shown in Fig. 3B and C, respectively.

### OR, INHIBIT, and XOR logic gates

Fig. 4 depicts the construction of OR, INHIBIT, and XOR logic gates. As shown in Fig. 4A, another common logic type, OR, is constructed, by also using $Hg^{2+}$ or $Ag^{+}$ as input. In an OR gate, the output of 1 is detected when either one or both of the two inputs is 1. The two padlock sequences (8) and (9) are hybridized with each other, and also hybridized with primers (10), respectively, to fabricate the supramolecular structure. The reaction of the supramolecular complex with either $Hg^{2+}$ or $Ag^{+}$ at 3′ end of corresponding padlock results in the ligation of respective padlock. Hence, in the presence of at least one of the two inputs, the RCA reaction should take place that is primed by corresponding primer in the 5′ to 3′ direction to perform the OR gate operation. The detailed reaction pathways, the fluorescence output and truth table of this gate activity is shown in Fig. S3.†

An INHIBIT gate is another notable type of logic operation due to its noncommutative behavior. In an INHIBIT logic, one input serves as a veto which has the power to disable the whole system. As illustrated in Fig. 4B, the INHIBIT logic gate is comprise of two padlock probes (11) and (12) which hybridize to each other with T–T mismatch at 5′ end of padlock (11) and C–C mismatch at 3′ end of padlock (12). When $Hg^{2+}$ is added, padlock (11) is ligated. Since the DNA polymerase Klenow fragment (exo-) used in this assay retains 5′ → 3′ polymerase activity, but has lost 5′ → 3′ and 3′ → 5′ exonuclease activities, the padlock (12) which still has a C–C mismatched site at 3′ end cannot serve as a primer for RCA. Otherwise, in the presence of $Ag^{+}$, the padlock (12) is circularized by DNA ligase, while padlock (11) has a 5′ end T–T mismatch. Thus, upon the addition of DNA polymerase/dNTPs, the RCA reaction proceeds by using padlock (11) as a primer from 5′-phosphate to 3′-OH end, which then produces a fluorescence signal. When the system is activated by the two ion-inputs, the padlocks (11) and (12) are circularized simultaneously, and hence, no strand can act as the primer for RCA. Thus, when only $Ag^{+}$ is present, the output is 1, otherwise it is 0. The experimental results of this system are presented in Fig. S4.†

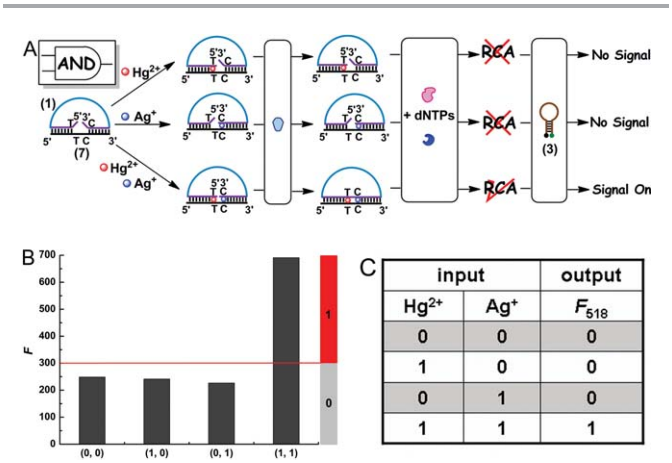


**Fig. 3** Diagrammatic representation (A), fluorescence results (B) and truth table (C) of "AND" logic gate that is activated by $Hg^{2+}$ and $Ag^{+}$ as inputs and connected to MB probes as reporters to generate fluorescence outputs.

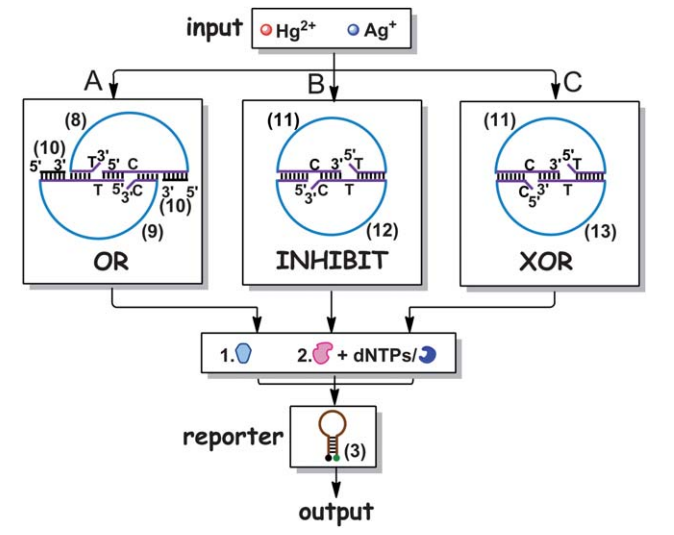


**Fig. 4** OR (A), INHIBIT (B), and XOR (C) logic gates are activated by $Hg^{2+}$ and $Ag^{+}$ as inputs and connected to MB probes as reporters to generate fluorescence outputs. The detailed diagrammatic representation, fluorescence results and truth table of each logic operation are shown in ESI.†

XOR (exclusive OR) Boolean behavior is outlined as Fig. 4C. In comparison with the above fabricated INHIBIT gate that has a C–C mismatch at the 3′ end of padlock (12), the C–C mismatch is at the 5′ end of padlock (13) in the XOR gate with the other components exactly the same. In accordance with the INHIBIT operation for $Ag^+$, the padlock (11) or (13) is respectively circularized by DNA ligase in the presence of either the $Hg^{2+}$ or $Ag^+$ input, leading to the performance of the RCA reaction by employing padlock (13) or (11) as primer and to the generation of fluorescence (true output). Otherwise, triggering the system with both inputs, $Hg^{2+}$ and $Ag^+$, results in the circularization of both padlocks (11) and (13) by DNA ligase. This prohibits the following RCA and the generation of fluorescence signals (false output). The fluorescence results are consistent with the XOR operation and the corresponding truth tables are presented in Fig. S5,† showing that fluorescence is triggered only upon activation by $Hg^{2+}$ or $Ag^+$ alone, and is extinguished in the presence of $Hg^{2+}$ and $Ag^+$.

### NAND, NOR, and XNOR logic gates

Moreover, we use the constructed AND, OR and XOR gates as platforms to design a NAND gate, a NOR gate and an XNOR gate, respectively, by using the double-stranded fluorescence probe in the NOT gate as the fluorescence output (Fig. 5, see ESI† for detail).

### Advanced logic devices

To demonstrate the flexibility and scalability of the proposed logic gates, the approach is then extended to advanced logic devices, half-adder (HA), half-subtractor (HS), and magnitude comparator systems. Also applying $Hg^{2+}$ and $Ag^+$ as inputs, the logic circuits composed of XOR and AND gates obtain an HA that produces Sum (S) and Carry (C) outputs, while the combination of XOR and INHIBIT gates generates an HS that produces Difference (D) and Borrow (B) outputs (Fig. 6). It should be noted that to enable the HA and HS to work, two kinds of MBs labeled with different fluorophore/quencher pairs are employed to generate the output of a single gate (FAM and Dabcyl of MB (3) for AND and INHIBIT, ROX and BHQ2 of MB (14) for XOR). In the HA system (Fig. 6A), in the absence of both inputs, the system doesn't work and neither fluorescence output is produced. In the presence of either input (and only one input), only the ROX fluorescence output ($\lambda = 608$ nm) is activated (the Sum bit output, the action of an XOR gate), while in the presence of both inputs, only the FAM fluorescence output ($\lambda = 518$ nm) is activated (the Carry bit output, the action of an AND gate). An HS is a more complicated circuit than HA, performing the subtraction "input B − input A" to account for the relative magnitudes of input A and input B. As shown in Fig. 6B, the Difference bit output as a result of "input B − input A" given by ROX ($\lambda = 608$ nm) is generated through the XOR gate, while the Borrow bit output in the case "input B < input A" given by FAM ($\lambda = 518$ nm) is generated through the INHIBIT gate. The fluorescence values resulting from the HA and HS operations and the corresponding truth tables are shown in Fig. 6.

A magnitude comparator is further constructed by combining XNOR and INHIBIT gates (Fig. 7). If both inputs are of equal binary magnitude (inputs are simultaneously present or absent, input A = input B), the output of XNOR gate fluorescently signalled by ROX tagged on MB (15) at 608 nm is true. If the inputs are not equal (input A > input B, or input A < input B), a false output of the XNOR is yielded. The superposed INHIBIT gate is employed to decide which one is greater, input A or input B. If input A < input B, the output of INHIBIT observed by the fluorescence signal of FAM at 518 nm is 1, whereas the output is 0. Thus, the three possible situations of inputs, A = B, A > B, and A < B can be easily distinguished in the magnitude comparator.

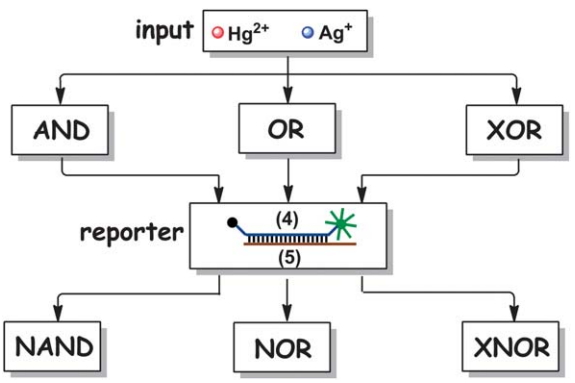


**Fig. 5** NAND, NOR, and XNOR logic gates are activated by $Hg^{2+}$ and $Ag^+$ as inputs and connected to double-stranded fluorescence probes as reporters to generate fluorescence outputs. The detailed diagrammatic representation, fluorescence results and truth table of each logic operation are shown in the ESI.†

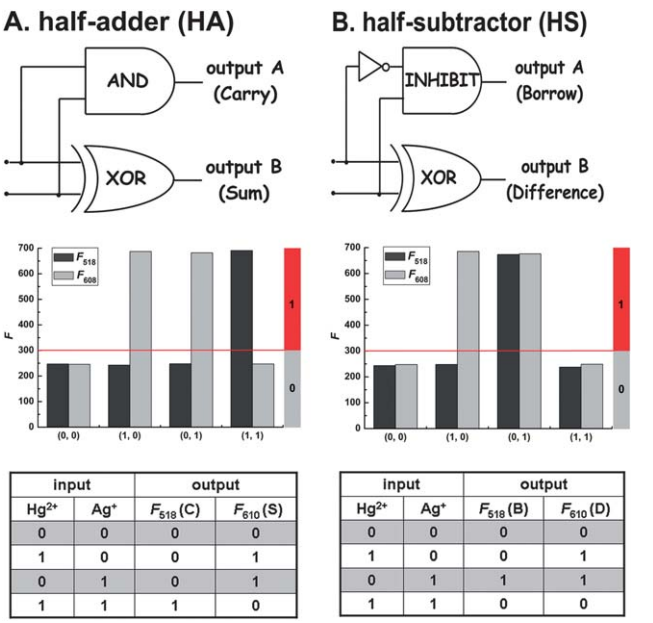


| input | | output | |
|---|---|---|---|
| $Hg^{2+}$ | $Ag^+$ | $F_{518}$ (C) | $F_{610}$ (S) |
| 0 | 0 | 0 | 0 |
| 1 | 0 | 0 | 1 |
| 0 | 1 | 0 | 1 |
| 1 | 1 | 1 | 0 |

| input | | output | |
|---|---|---|---|
| $Hg^{2+}$ | $Ag^+$ | $F_{518}$ (B) | $F_{610}$ (D) |
| 0 | 0 | 0 | 0 |
| 1 | 0 | 0 | 1 |
| 0 | 1 | 1 | 1 |
| 1 | 1 | 0 | 0 |

**Fig. 6** Symbolisation, fluorescence results, and truth table of the half-adder (HA) (A) and half-substractor (HS) (B). The XOR logic operation for output Sum (S) in HA is the same as that for output Difference (D) in HS.

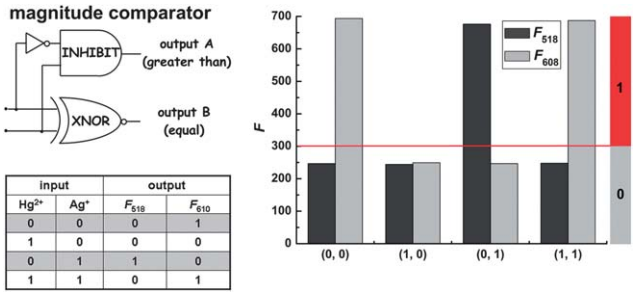


| input | | output | |
|---|---|---|---|
| $Hg^{2+}$ | $Ag^{+}$ | $F_{518}$ | $F_{610}$ |
| 0 | 0 | 0 | 1 |
| 1 | 0 | 0 | 0 |
| 0 | 1 | 1 | 0 |
| 1 | 1 | 0 | 1 |

**Fig. 7** Symbolisation, fluorescence results, and truth table of magnitude comparator.

## Conclusions

In summary, the specific interactions of metal ions ($Hg^{2+}$ or $Ag^{+}$) with mismatched base pairs (T–T or C–C) are ingeniously applied to trigger DNA ligase activity to perform an RCA reaction. This strategy is achieved for highly sensitive and selective detection of $Hg^{2+}$ (0.1 nM) and $Ag^{+}$ (0.1 nM). Moreover, a complete set of logic gates are constructed by using $Hg^{2+}$ and $Ag^{+}$ as inputs and RCA products as outputs. Two kinds of fluorescence probes provide read-out signals for the logic operations: molecular beacon probe for OR, AND, INHIBIT, XOR gates, and double-stranded fluorescence probe for NOR, NAND, and XNOR gates. By combining particular gates, three advanced logic devices, such as a half-adder (AND/XOR combination), a half-subtractor (XOR/INHIBIT combination), and a magnitude comparator (XNOR/INHIBIT combination), are successfully demonstrated. It is believable that our study not only introduces a new concept for detecting metal ions and devising molecular logic gates but also provides a new insight into the development of analytical science and nanotechnology. For example, by combining with other novel technologies, such as aptamer recognition, the proposed assay might be applicable to the design of molecular translator and detection of other targets.

## Experimental section

### Chemicals and regents

The used oligonucleotides were synthesized by Sangon Biotechnology Co., Ltd. (Shanghai, China). The sequences are shown in Table 1. T4 DNA ligase, DNA polymerase Klenow fragment (exo-), and the mixture of deoxyribonucleoside 5′-triphosphates (dNTPs) were purchased from Beijing Transgen Biotech Co., Ltd. (Beijing, China), Fermentas (Canada), and SBS Genetech Co., Ltd. (Beijing, China), respectively. Cysteine (Cys) was obtained from Sangon Biotechnology Co., Ltd. (Shanghai, China). All reagents were of analytical grade and used as received without further purification. Double-distilled, deionized water was used throughout the experiments.

### YES and NOT gates for $Hg^{2+}$ detection

For $Hg^{2+}$ detection in a YES gate, a 10 μL of 1.0 μM padlock probe (1) and a 10 μL of 1.0 μM primer (2) were mixed and heated at 90 °C for 5 min, and gradually cooled to 4 °C. To this mixture was added equal volume of $Hg^{2+}$ solution with different concentrations, allowing interaction for 1 h to form the T–$Hg^{2+}$–T base pairs. Then, 8.0 μL of T4 buffer (250 mM Tris–HCl, pH 7.5, 50 mM $MgCl_2$, 5 mM DTT, 5 mM ATP, 125 μg $mL^{-1}$ BSA, and Enhancer) and 2.0 μL of T4 DNA ligase (200 units per μL) were added, followed by incubating overnight. Then, 7.0 μL of dNTPs (10 mM), 5.5 μL of DNA polymerase Klenow fragment (exo-) buffer (500 mM Tris–HCl, pH 8.0, 50 mM $MgCl_2$, 10 mM DTT), 2.5 μL of DNA polymerase Klenow fragment (exo-) (10 U $\mu L^{-1}$), and 5 μL of Cys (4.0 μM) were added to perform the RCA reaction at 37 °C for 1 h. Subsequently, the resulting solution was incubated at 0 °C for 10 min to inactivate the DNA polymerase Klenow fragment (exo-). Then, the molecular beacon (MB) probes were added and allowed to hybridize with the resulting RCA products for 1 h. Then fluorescence spectra were recorded on a Hitachi F-4600 fluorescence spectrophotometer (Tokyo, Japan). For $Hg^{2+}$ detection in a NOT gate, the double-stranded fluorescent probes were prepared by annealing and used to

**Table 1** Oligonucleotide sequences used in this work

| No. | Sequence (5′ to 3′) |
|---|---|
| (1) | P-TGTGAGGTAGAAAAAAGCCGATGAGGGAAGAAAAAAAAGACGAGAGAC |
| (2) | CTACCTCACTGTCTCTCGTC |
| (3) | FAM-AGCTAAGCCGATGAGGGAAGAATTAGCT-Dabcyl |
| (4) | FAM-AGCTATTTCTTCCCTCATCGGCATAGCT-Dabcyl |
| (5) | GCCGATGAGGGAAGAAAAAAAAGACGAG |
| (6) | CTACCTCACACTCTCTCGTC |
| (7) | CTACCTCACTCTCTCTCGTC |
| (8) | P-CCACGCGCTGGCGAGACGCGAGGAATAGAAAAAAGCCGATGAGGGAAGAAAAAAAAGACGAGAAGACGTGGT |
| (9) | P-CGCGTGGTCCACGTCACGCGAGGAATAGAAAAAAGCCGATGAGGGAAGAAAAAAAAGACGAGAACTCGCCAC |
| (10) | CCTCGCGT |
| (11) | P-TGGTGCAGTAGAAAAAAGCCGATGAGGGAAGAAAAAAAAGACGAGAGCGAGTCGCGCACC |
| (12) | P-ACTCGCTTAGAAAAAAGCCGATGAGGGAAGAAAAAAAAGACGAGCTGCACCTGGTGCGCC |
| (13) | P-CACTCGCTTAGAAAAAAGCCGATGAGGGAAGAAAAAAAAGACGAGCTGCACCTGGTGCGC |
| (14) | ROX-AGCTAAGCCGATGAGGGAAGAATTAGCT-BHQ2 |
| (15) | ROX-AGCTATTTCTTCCCTCATCGGCATAGCT-BHQ2 |

hybridize with RCA products for 1 h. Other steps were carried out as for the YES gate.

### Logic operations

Firstly, corresponding oligonucleotide strands were mixed and annealed to fabricate supramolecular structures. For AND, OR, XOR, and INHIBIT logic operations, other steps were carried out as for the YES gate. For NOR, XNOR, and NAND logic operations, other steps were carried out as for the NOT gate.

## Acknowledgements

This work was supported by the National Natural Science Foundation of China (21105052, 21121091), the Program for New Century Excellent Talents in University of Ministry of Education of China (NCET-12-1024), the China Postdoctoral Science Foundation (2012M510130) and National Basic Research Program of China (2011CB933502).



## Notes and references

1 (*a*) I. Onyido, A. R. Norris and E. Buncel, *Chem. Rev.*, 2004, **104**, 5911–5929; (*b*) T. A. Baughman, *Environ. Health Perspect.*, 2006, **114**, 147–152.

2 (*a*) D. T. Quang and J. S. Kim, *Chem. Rev.*, 2010, **110**, 6280–6301; (*b*) H. N. Kim, W. X. Ren, J. S. Kim and J. Yoon, *Chem. Soc. Rev.*, 2012, **41**, 3210–3244; (*c*) Y. Xiang and Y. Lu, *Chem. Commun.*, 2013, **49**, 585–587.

3 (*a*) R. R. Breaker, *Nat. Biotechnol.*, 1997, **15**, 427–431; (*b*) Y. Lu and J. Liu, *Curr. Opin. Biotechnol.*, 2006, **17**, 580–588; (*c*) I. Willner, B. Shlyahovsky, M. Zayats and B. Willner, *Chem. Soc. Rev.*, 2008, **37**, 1153–1165.

4 (*a*) A. Ono and H. Togashi, *Angew. Chem., Int. Ed.*, 2004, **43**, 4300–4302; (*b*) Y. Miyake, H. Togashi, M. Tashiro, H. Yamaguchi, S. Oda, M. Kudo, Y. Tanaka, Y. Kondo, R. Sawa, T. Fujimoto, T. Machinami and A. Ono, *J. Am. Chem. Soc.*, 2006, **128**, 2172–2173.

5 (*a*) A. Ono, S. Cao, H. Togashi, M. Tashiro, T. Fujimoto, T. Machinami, S. Oda, Y. Miyake, I. Okamoto and Y. Tanaka, *Chem. Commun.*, 2008, 4825–4827; (*b*) T. Li, L. Shi, E. Wang and S. Dong, *Chem.–Eur. J.*, 2009, **15**, 3347–3350.

6 (*a*) G. Mor-Piperberg, R. Tel-Vered, J. Elbaz and I. Willner, *J. Am. Chem. Soc.*, 2010, **132**, 6878–6879; (*b*) Y. Wen, F. Xing, S. He, S. Song, L. Wang, Y. Long, D. Li and C. Fan, *Chem. Commun.*, 2010, **46**, 2596–2598; (*c*) M. Stobiecka, A. A. Molinero, A. Chalupa and M. Hepel, *Anal. Chem.*, 2012, **84**, 4970–4978; (*d*) D. Li, A. Wieckowska and I. Willner, *Angew. Chem., Int. Ed.*, 2008, **47**, 3927–3931.

7 (*a*) T. Li, E. Wang and S. Dong, *J. Am. Chem. Soc.*, 2009, **131**, 15082–15083; (*b*) C.-W. Liu, C.-C. Huang and H.-T. Chang, *Anal. Chem.*, 2009, **81**, 2382–2387; (*c*) M. Moshe, J. Elbaz and I. Willner, *Nano Lett.*, 2009, **9**, 1196–1200; (*d*) S. Bi, Y. Yan, S. Hao and S. Zhang, *Angew. Chem., Int. Ed.*, 2010, **49**, 4438–4442; (*e*) J. Elbaz, O. Lioubashevski, F. Wang, F. Remacle, R. D. Levine and I. Willner, *Nat. Nanotechnol.*, 2010, **5**, 417–422.

8 R. Freeman, T. Finder and I. Willner, *Angew. Chem., Int. Ed.*, 2009, **48**, 7818–7821.

9 K. S. Park, C. Jung and H. G. Park, *Angew. Chem., Int. Ed.*, 2010, **49**, 9757–9760.

10 (*a*) W. Zhao, M. M. Ali, M. A. Brook and Y. Li, *Angew. Chem., Int. Ed.*, 2008, **47**, 6330–6337; (*b*) M. Stougaard, S. Juul, F. F. Andersen and B. R. Knudsen, *Integr. Biol.*, 2011, **3**, 982–992.

11 (*a*) C. Larsson, I. Grundberg, O. Söderberg and M. Nilsson, *Nat. Methods*, 2010, **7**, 395–397; (*b*) Z.-S. Wu, S. Zhang, H. Zhou, G.-L. Shen and R. Yu, *Anal. Chem.*, 2010, **82**, 2221–2227.

12 J. Lee, K. Icoz, A. Roberts, A. D. Ellington and C. A. Savran, *Anal. Chem.*, 2010, **82**, 197–202.

13 (*a*) W. Cheng, L. Ding, Y. Chen, F. Yan, H. Ju and Y. Yin, *Chem. Commun.*, 2010, **46**, 6720–6722; (*b*) H. Ji, F. Yan, J. Lei and H. Ju, *Anal. Chem.*, 2012, **84**, 7166–7171.

14 (*a*) Y. Cheng, X. Zhang, Z. Li, X. Jiao, Y. Wang and Y. Zhang, *Angew. Chem., Int. Ed.*, 2009, **48**, 3268–3272; (*b*) S. Neubacher and C. Arenz, *ChemBioChem*, 2009, **10**, 1289–1291; (*c*) S. Bi, Y. Cui and L. Li, *Analyst*, 2013, **138**, 197–203.

15 (*a*) W. Xu, X. Xie, D. Li, Z. Yang, T. Li and X. Liu, *Small*, 2012, **8**, 1846–1850; (*b*) Y. Zhao, L. Qi, F. Chen, Y. Dong, Y. Kong, Y. Wu and C. Fan, *Chem. Commun.*, 2012, **48**, 3354–3356.

16 (*a*) Q. Xue, L. Wang and W. Jiang, *Chem. Commun.*, 2012, **48**, 3930–3932; (*b*) S. Bi, L. Li and S. Zhang, *Anal. Chem.*, 2010, **82**, 9447–9454.

17 (*a*) E. J. Cho, L. Yang, M. Levy and A. D. Ellington, *J. Am. Chem. Soc.*, 2005, **127**, 2022–2023; (*b*) A. Cao and C.-Y. Zhang, *Anal. Chem.*, 2012, **84**, 6199–6205.

18 J.-S. Lee, P. A. Ulmann, M. S. Han and C. A. Mirkin, *Nano Lett.*, 2008, **8**, 529–533.